OPEN ACCESS Freely available online

PLoS one

Growth, Structure and Spectroscopic Characterization of Nd^{3+}-Doped $KBaGd(WO_4)_3$ Crystal with a Disordered Structure

Bin Xiao[1,2], Yisheng Huang[1], Lizhen Zhang[1], Zhoubin Lin[1], Guofu Wang[1]*

1 Key Laboratory of Optoelectronics Material Chemistry and Physics, Fujian Institute of Research on the Structure of Matter, Chinese Academy of Sciences, Fuzhou, Fujian, China, **2** Graduate School of Chinese Academy of Sciences, Beijing, China

Abstract

The undoped and the Nd^{3+}:$KBaGd(WO_4)_3$ crystals were grown by the top seeded solution growth (TSSG) method from a flux of $K_2W_2O_7$. The structure of the pure crystal was determined by the single-crystal X-ray diffraction method. It crystallizes in the monoclinic symmetry with space group *C*2/*c*. In the structure, K^+ and Ba^{2+} ions share the same 8*f* site with occupancy of 0.464 and 0.536, respectively. The investigation of spectral properties of Nd^{3+}:$KBaGd(WO_4)_3$ crystal indicates that it exhibits broad absorption and emission bands, which are attributed to locally disordered environments around the Nd^{3+} centers. The broad absorption band is suitable for diode laser pumping.

Citation: Xiao B, Huang Y, Zhang L, Lin Z, Wang G (2012) Growth, Structure and Spectroscopic Characterization of Nd^{3+}-Doped $KBaGd(WO_4)_3$ Crystal with a Disordered Structure. PLoS ONE 7(7): e40229. doi:10.1371/journal.pone.0040229

Editor: Matthew Shawkey, University of Akron, United States of America

Received December 14, 2011; **Accepted** June 3, 2012; **Published** July 6, 2012

Funding: This work is supported by the National Natural Science Foundation of China (No. 61108054) and the National Natural Science Foundation of Fujian Province (No. 2011J01376), respectively. The funders had no role in study design, data collection and analysis, decision to publish, or preparation of the manuscript.

Competing Interests: The authors have declared that no competing interests exist.

* E-mail: wgf@ms.fjirsm.ac.cn

Introduction

The diode-laser pumped solid-state lasers are useful in a wide variety of applications in the fields of military [1,2], industry [3] and medical treatments [4] due to their advantages, such as outstanding stability, high efficiency, compact size and long lifetime. A lot of well-known Nd^{3+}-doped laser crystals (Nd:YAG, for example [5]) are commercially available, however, they can be hardly pumped with diode-lasers. Because they have very narrow absorption bands near their pumped wavelength compared to the emission bandwidths of common diode-lasers (several nanometers), they cannot absorb the pump energy of diode-lasers efficiently. Besides, the temperature stability of the emission wavelength of diode-lasers needs to be crucially controlled for laser crystals with narrow absorption bands, since the emission wavelength of the diode-lasers changes at 0.2–0.3 nm/K with the operating temperature of the laser device. [6] As a consequence, it is necessary to explore novel laser crystals with large absorption bandwidths for diode pumping.

The broadening of the spectral features can be expected for solid-state materials with multisites, defects, or local disorder [7]. In the past few years, there have been a lot of studies on the family of scheelite-related disordered molybdate and tungstate crystals $AT(XO_4)_2$ (A = monovalent Li, Na; T = trivalent Bi, Y, La-Lu; X = Mo, W) [8–10]. These disordered crystals have been demonstrated as promising materials in the domains of tunable and ultrashort femto-second laser pulse due to the obvious advantage of large spectral broadening. Recently, we synthesized a new triple tungstate $KBaGd(WO_4)_3$ compound also with disordered structure. Because of the mixed K(Ba) occupancy of the same crystallographic site, 8*f*, the structure of $KBaGd(WO_4)_3$ presents some local disorder around Gd^{3+} sites, and thus can lead to the spectral broadening when rare-earth luminescent ions (such as Nd^{3+}) replace Gd^{3+}. Therefore, this paper reports on the growth, structure and spectral properties of Nd^{3+}-doped $KBaGd(WO_4)_3$ crystal.

Materials and Methods

1.Synthesis and Crystal Growth

Polycrystalline samples of undoped $KBaGd(WO_4)_3$ were synthesized by means of the solid-state reaction method. The synthesis process followed that of ref. [11]. To evaluate melting point of the synthesized $KBaGd(WO_4)_3$ compound, the thermal analysis was carried out by differential scanning calorimetry (DSC) using a NETZCH STA 499C Simultaneous Thermal Analyzer, which was performed up to 1563 K at a heating and cooling rate of 15 K min^{-1}.

The undoped and Nd^{3+}:$KBaGd(WO_4)_3$ crystals were grown by the top seeded solution growth method. The crystal growth was carried out in a vertical tubular furnace, as shown in Fig. 1. An AL-708 controller with controlling accuracy of ±0.1 K was used to control the furnace temperature and the cooling rate.

2.Crystal Structure Analysis

A single crystal of undoped $KBaGd(WO_4)_3$ with dimensions of $0.10\times0.10\times0.10$ mm^3 was selected for X-ray diffraction determinations. The diffraction data were collected on a Mercury70 CCD diffractometer equipped with graphite-monochromated Mo Kα (λ = 0.71073 Å) radiation at 293 K. A total of 1214 independent reflections were collected in the range of $3.35° < \theta < 27.45°$, of

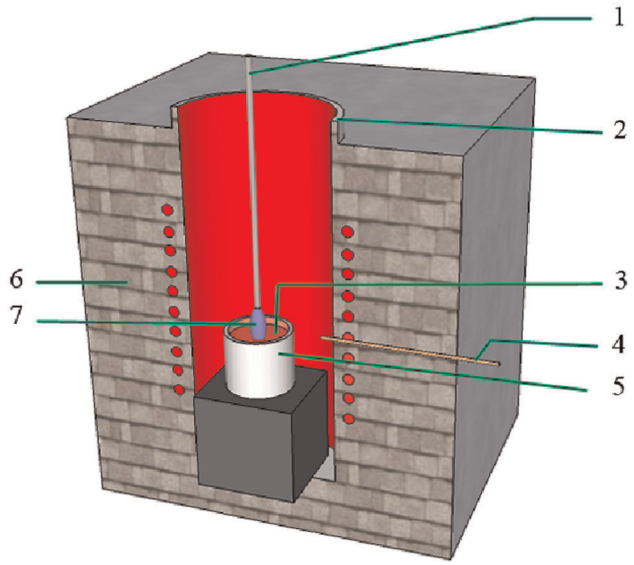

Figure 1. Schematic diagram of crystal growth apparatuses: (1) seed holder; (2) Al_2O_3 tube; (3) melt; (4) thermocouple; (5) crucible; (6) thermal insulation material; (7) seed.
doi:10.1371/journal.pone.0040229.g001

which 1102 with $I \geq 2\sigma(I)$ were independent. The absorption correction based on the empirical PSI-scan technique was applied. The structure was solved by direct methods and refined by the full-matrix least squares technique with the SHELXL97 program package [12]. The final unweighted residual factor R which is used to judge the structure model is 0.0229. The weighted residual factor wR is 0.0514 with the weighting factor w:

$$w = 1/[\sigma^2(F_o^2) + (0.0268P)^2 + 0.0000P],$$

$$\text{where } P = (F_o^2 + 2F_c^2)/3,$$

in the above equations, $\sigma(F_o^2)$ is the estimated standard uncertainty of the observed reflections, F_o^2 and F_c^2 means the observed and calculated squared structure factors, respectively. After the refinement, the residual electron density $(\Delta\rho)_{max} = 1.542$, and $(\Delta\rho)_{min} = -2.045$ e/Å^3, $(\Delta/\sigma)_{max} = 0.000$. The value of goodness of fit S which is used to adjust the weighting scheme is 1.050. The details of the X-ray structure analysis are listed in (Table S1). The X-ray power diffraction (XRD) pattern of undoped $KBaGd(WO_4)_3$ was determined using a D-max-rA type diffractometer with Cu Kα radiation ($\lambda = 1.54056$ Å) at room temperature. The power electron diffraction pattern of undoped $KBaGd(WO_4)_3$ crystal which was carried out by a JEM-2010 transmission electron microscope.

3.Spectral Characterization

Since Nd^{3+}:$KBaGd(WO_4)_3$ crystal with the monoclinic system is optically biaxial, three optical indicatrix axes (X, Y, Z) should be determined before the measurement of polarized spectra. One of the optical indicatrix axes (Y) is parallel to the unique two-fold crystallographic axis (b-axis, which is also the C_2 symmetry axis), and the other two lie in a perpendicular plane to this axis. The orientation of the crystal was performed by means of crossed polarized microscope, and the orientating procedure follows that of ref. [13]. The c-axis is at 16° anticlockwise with respect to the indicatrix Z-axis, and the angular relationship between the optical

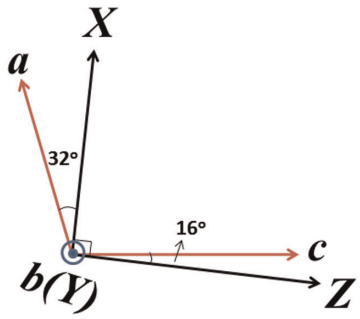

Figure 2. Relative orientation between the optical indicatrix axes (X, Y, Z) and the crystallographic axes (a, b, c) of the Nd^{3+}:$KBaGd(WO_4)_3$ crystal. The plot means view from the positive b-axis direction.
doi:10.1371/journal.pone.0040229.g002

indicatrix axes and the crystallographic axes (a, b, c) for Nd^{3+}:$KBaGd(WO_4)_3$ crystal is shown in Fig. 2. After orientation, a sample with dimensions of $5.5 \times 3.8 \times 2.6$ mm^3 and high optical quality was cut from the as-grown crystal, as shown in Fig.3 (c).

The polarized absorption spectra were measured with a Perkin-Elmer UV-VIS-NIR spectrophotometer (Lambda 900). Excited by a continuous Xe-lamp at 805 nm, the polarized emission spectra were recorded using an Edinburgh Instruments FLS920 spectrophotometer. All the spectral experiments were carried out at room temperature. In spectral experiment, the electric field of the light is parallel to each one of the three optical indicatrix axes, $E||X$, $E||Y$, and $E||Z$.

Results and Discussion

1.DSC Analysis and Crystal Growth

The DSC result reveals that the undoped $KBaGd(WO_4)_3$ crystal melts incongruently (Fig. 4). In the heating cycle, an endothermic peak corresponding to a solid-liquid transformation is observed, which means the $KBaGd(WO_4)_3$ is decomposed at 1372 K, and then melts completely to form the liquid phase at 1477 K. The cooling curve shows two exothermic peaks with maxima at 1463 K and 1355 K, respectively, with the second one corresponding to resolidification of $KBaGd(WO_4)_3$.

Since the $KBaGd(WO_4)_3$ crystal exists a phase transition at temperatures lower than the melting point, hence the best technique to grow it is the top seeded solution growth method (TSSG) [14]. The Nd^{3+}:$KBaGd(WO_4)_3$ crystal was grown in a flux of $K_2W_2O_7$ by the this method, where the molar ratio of $KBaGd(WO_4)_3$ to $K_2W_2O_7$ is 1:1. The chemical used were K_2CO_3, $BaCO_3$, WO_3 with analytical-grade as well as Gd_2O_3 and Nd_2O_3 with 99.99% purity. According to their stoichiometric composition, 3.0 at % Nd^{3+}-doped $KBaGd(WO_4)_3$ and $K_2W_2O_7$ were weighed. The weighed materials were mixed and put in a platinum crucible with a volume of 100 mm^3. The mixture was slowly heated up to 1273 K in air atmosphere, and then maintained at that temperature for 48 hours to achieve a homogeneous melt. The saturation temperature of the solution was determined by repeated seeding. The starting growth temperature was about 1203 K. The crystals were grown at a cooling rate of 1K/day and a rotating rate of 45 rpm. When the growth ended, the grown crystals were carefully withdrawn from the solution and cooled to room temperature at 15 K h^{-1}. The Nd^{3+}:$KBaGd(WO_4)_3$ crystal with few inclusions and dimensions of $21 \times 24 \times 12$ mm^3 was obtained, as shown in Fig. 3(a). The morphology of the crystal is shown in Fig. 3(b), which was

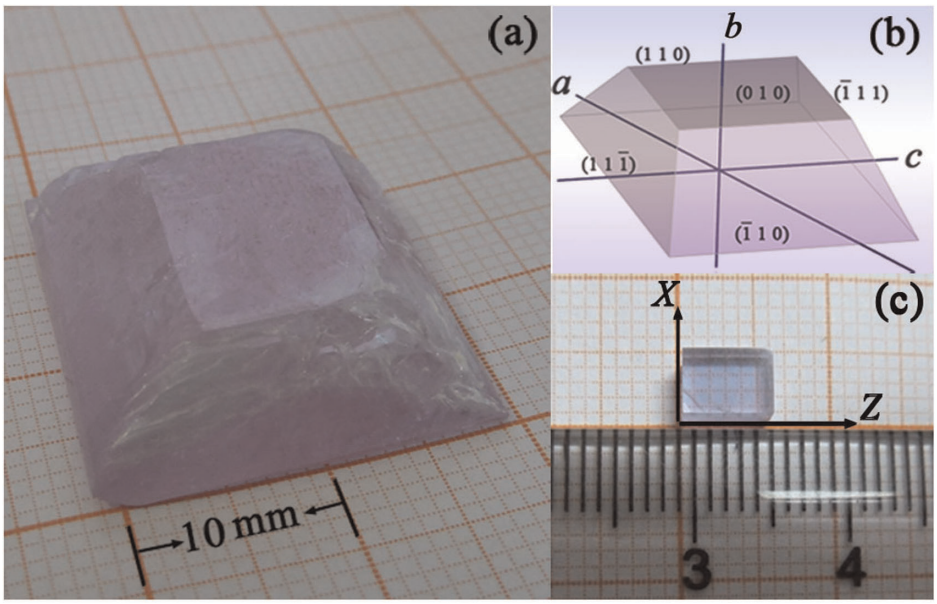

Figure 3. (a) Nd^{3+}:$KBaGd(WO_4)_3$ crystal grown by TSSG method. (b) Stimulated facets marked by Miller indices (hkl). (c) An orientated rectangle sample cut from the as-grown crystal. Each face is perpendicular to one of the optical indicatrix axes.
doi:10.1371/journal.pone.0040229.g003

simulated with Bravais-Friedel and Donnay-Harker based *WinX-Morph* software. [15].

The composition of the grown crystal was measured in an inductively coupled plasma by atomic emission spectrometry (ICP-AES) technique. For this purpose, the Nd^{3+}:$KBaGd(WO_4)_3$ sample was heated at 363 K and dissolved in 37% HCl, then the signal of ICP intensity was quantified from the comparison of the standard elements and corrected by the calibration curve. The result of ICP is listed in Table 1. The measured molar ratio K: Ba: (Gd+Nd): W is close to 1:1:1:3, which agrees with the composition of Nd^{3+}:$KBaGd(WO_4)_3$ compounds.

2.Crystal Structure

Fig. 5(a) shows the XRD pattern of undoped $KBaGd(WO_4)_3$ crystal that can be indexed on the basis of lattice parameters. The indexed result of power electron diffraction pattern of undoped $KBaGd(WO_4)_3$ crystal is in agreement with that of the powder X-ray diffraction pattern, as shown in Fig. 5(b), which confirmed the XRD result. The powder XRD data of undoped $KBaGd(WO_4)_3$ crystal are listed in Table S2.

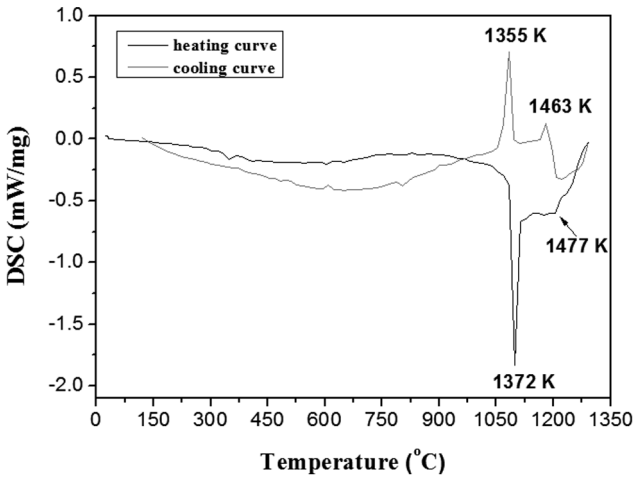

Figure 4. DSC curves of undoped $KBaGd(WO_4)_3$ compound.
doi:10.1371/journal.pone.0040229.g004

The crystallographic analysis of the undoped $KBaGd(WO_4)_3$ crystal reveals that it crystallizes in the monoclinic system with space group $C2/c$. The lattice parameters of $KBaGd(WO_4)_3$ crystal are: $a = 17.544(4)$ Å, $b = 12.1742(16)$ Å, $c = 5.3202(9)$ Å, $\beta = 105.498(11)^\circ$, and $V = 1095.0(3)$ Å^3 (also see CIF file: CIF S1). The atomic coordinates and thermal parameters are given in Table S3. In the refined structure, the Gd and W(2) fully occupy 4*e* sites, and W(1) as well as the eight types of O are found in different 8*f* sites. After least-squares refinement, the valence charge equilibrium and the magnitude of temperature factors demonstrate the existence of a statistic distribution of K and Ba, in single 8*f* site with occupancy factors fixed to 0.464:0.536, which shows that $KBaGd(WO_4)_3$ crystal has a high disordered structure.

The crystalline structure is constituted by K/BaO_8 distorted square antiprisms with C_1 symmetry, distorted GdO_8 polyhedra which form chains lying along the *c*-axis (see Fig. 6 (a)) and two kinds of distorted WO_4 tetrahedra. It can be described as layers stacked along the *a*-axis formed by corrugated six-membered rings of disordered K/BaO_8 polyhedra, which share edges (Fig. 6 (b)). Adjacent layers are connected through distorted WO_4 polyhedra and GdO_8 chains (Fig. 7). The distinctive layered arrangement further increases the locally variable crystal field around Gd sites. The Gd^{3+} ions could provide appropriate sites for Nd^{3+} replacements because the Gd^{3+} and Nd^{3+} ions have the same valence, and additionally offer multiple distributions of cationic environments around these sites due to the coexistence of K^+, Ba^{2+} and Gd^{3+} ions. Therefore, when Nd^{3+} replaces Gd^{3+} ions, the high disordered environment around the Nd^{3+} dopant ions leads to inhomogeneous broadening of the absorption and emission bands [16,17].

Table 1. Summary of the elemental analysis results of 3.08 at% Nd^{3+}-doped $KBaGd(WO_4)_3$ crystal by the ICP-AES technique.

				(Gd+Nd)[a]	
Elements	**W**	**K**	**Ba**	**Gd**	**Nd**
Required (Wt%)	51.22	3.63	12.75	14.02	0.54
Measured (wt%)	50.96±1.02	3.27±0.07	12.43±0.25	13.84±0.28	0.43±0.009
Calculated molar number (10^{-2})	27.72±0.55	8.36±0.18	9.05±0.18	8.80±0.18	0.30±0.006
Molar ratio	3.06±0.12	0.92±0.038	1±0.04	0.97±0.039	0.0309±0.0013
				(Gd+Nd) ≈ 1	

[a]the Gd^{3+} ions were generally substituted by Nd^{3+} ions in the Nd^{3+}-doped $KBaGd(WO_4)_3$ crystal because the Gd^{3+} and Nd^{3+} ions have the same valence.
doi:10.1371/journal.pone.0040229.t001

3.Spectral Properties

Fig. 8 shows the polarized absorption spectra of the Nd^{3+}-doped $KBaGd(WO_4)_3$ at room temperature. These absorption lines are due to transition from the ground state $^4I_{9/2}$ to the various excited states of Nd^{3+} ions. In the absorption spectra, the most interesting is the broad absorption bands in the range of 780–840 nm, which is close to the output wavelength of commercially diode laser devices. The absorption spectra are strong polarization dependent because of the anisotropy of the monoclinic crystal. The absorption spectrum for $E||Y$ polarization is strongest among the three absorption spectra and it has a full-width at half-maximum (FWHM) of 14 nm at 803 nm, which is larger than that of the ordered crystal, like Nd^{3+}:$BaGd_2(MoO_4)_4$ crystal (4 nm, $E||Z$) or LaB_3O_6 (5 nm, $E||X$) [18,19]. Such large FWHM caused by the highly disordered structure around Nd^{3+} centers is suitable for diode-laser pumping. This demonstrates the Nd^{3+}-doped $KBaGd(WO_4)_3$ crystal can be pumped effectively and not restricted to the temperature stability of the output wavelength of diode-laser.

The absorption cross-section σ_a was calculated using $\sigma_a = \alpha/N_c$ formula, where α is the absorption coefficient and N_c is the concentration of Nd^{3+}. The concentration of Nd^{3+} ions in Nd^{3+}:$KBaGd(WO_4)_3$ crystal was measured to be 3.08 at% (i.e. 1.12×10^{-20} cm^{-3}), and the results of the σ_a are listed in Table 2.

The emission cross-sections were calculated using the Füchtbauer-Ladenbrug (F-L) equation, [20].

$$\sigma_e^q = \frac{\lambda^5 A_q (J - J') I_q(\lambda)}{8\pi c n^2 \int_q (\lambda) \mathrm{d}\lambda} \quad (1)$$

where $I_q(\lambda)$ is the emission intensity at wavelength λ with q polarization, A_q is the emission probability which can be calculated from the Judd-Ofelt theory [21,22], the refractive index n is calculated to be 1.83 using the method mentioned in Ref. [23].

Fig. 9 shows the wavelength dependences of the stimulated emission cross-sections. Three emission bands observed at 850–950, 1020–1150 and 1300–1450 nm are due to the transitions of $^4F_{3/2} \rightarrow {}^4I_{9/2}$, $^4F_{3/2} \rightarrow {}^4I_{11/2}$ and $^4F_{3/2} \rightarrow {}^4I_{13/2}$, respectively. The most important transition of $^4F_{3/2} \rightarrow {}^4I_{11/2}$ is centered at about 1060 nm. The FWHM for $E||Y$ polarization is 24 nm, which is much larger than that of ordered structure crystals (see Table 2). The peak stimulated emission cross-sections for the transition of $^4F_{3/2} \rightarrow {}^4I_{11/2}$ are 4.5, 6.5 and 4.1×10^{-20} cm^2 for $E||X$, $E||Y$ and $E||Z$, respectively.

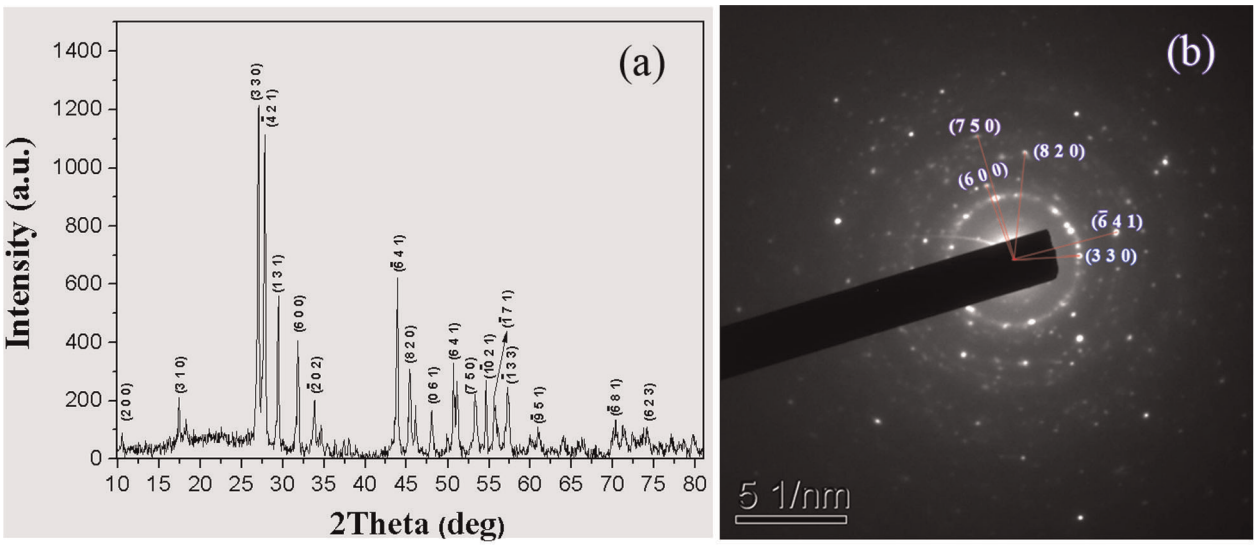

Figure 5. (a) Powder XRD patterns of undoped $KBaGd(WO_4)_3$ crystal. (b) Powder electron diffraction pattern of the undoped $KBaGd(WO_4)_3$ crystal.
doi:10.1371/journal.pone.0040229.g005

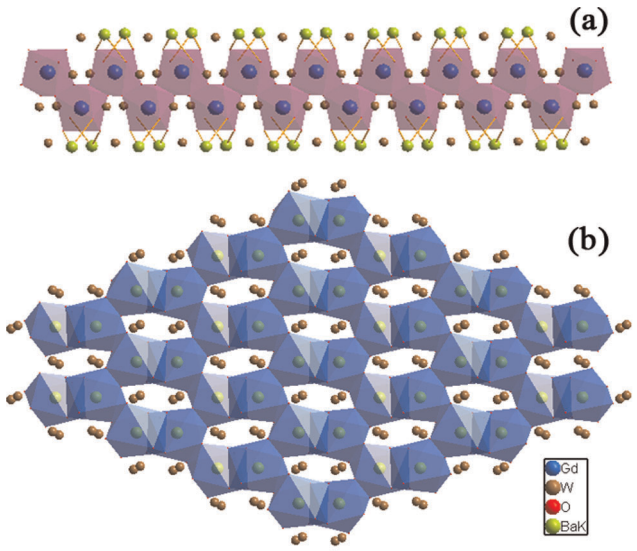

Figure 6. View of the *ab* plane of the $KBaGd(WO_4)_3$ crystal. (a) Chain formed by GdO_8 disordered polyhedra. (b) Six-membered rings of square antiprisms K/BaO_8.
doi:10.1371/journal.pone.0040229.g006

4.Conclusion

The 3.08 at% Nd^{3+}-doped $KBaGd(WO_4)_3$ crystal was successfully grown by the TSSG method. The thermal analysis shows it melts incongruently at 1372 K. The structure analysis indicates that the undoped $KBaGd(WO_4)_3$ crystal has a statistic distribution of K(0.464) and Ba(0.536) atoms. Each Ba(K) is coordinated by eight oxygen atoms to form a distorted polyhedron. This fact and its layered arrangement structure lead to locally disordered environments around the Gd^{3+} ions. When Gd^{3+} ions are substituted by Nd^{3+} dopant ions, the disordered structure results the broad FWHM of absorption and emission bands. Such broad FWHM of absorption band is suitable for diode-laser pumping. The Nd^{3+}:$KBaGd(WO_4)_3$ crystal with broad FWHM of emission band is promising as a candidate for tunable and short pulse solid-state laser operation. The spectroscopic properties of the Nd^{3+}:$KBaGd(WO_4)_3$ crystal are anisotropic with the largest absorption and emission cross sections for $E||Y$ polarization. The Nd^{3+}:$KBaGd(WO_4)_3$ crystal has large absorption and emission cross-sections, which are 6.9×10^{-20} cm^2 at 805 nm and 6.5×10^{-20} cm^2 at 1060 nm respectively.

Supporting Information

Table S1 Crystal data and structure refinement details for undoped $KBaGd(WO_4)_3$.
(DOC)

Table S2 Powder XRD data of undoped $KBaGd(WO_4)_3$ crystal.
(DOC)

Table S3 Atomic coordinates and thermal parameters for undoped $KBaGd(WO_4)_3$ crystal.
(DOC)

CIF S1 The CIF file of the undoped $KBaGd(WO_4)_3$ crystal.
(CIF)

Author Contributions

Conceived and designed the experiments: BX GW. Performed the experiments: BX ZL. Analyzed the data: BX GW. Contributed reagents/materials/analysis tools: YH LZ. Wrote the paper: BX GW.

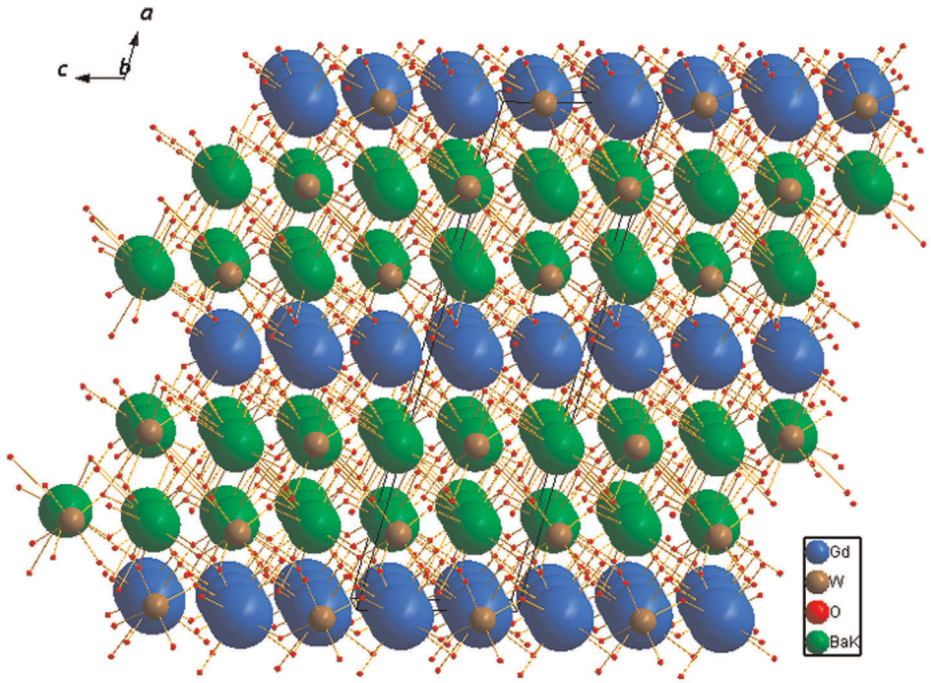

Figure 7. View along the *ac* plane shows the layers stacked along the *a*-axis.
doi:10.1371/journal.pone.0040229.g007

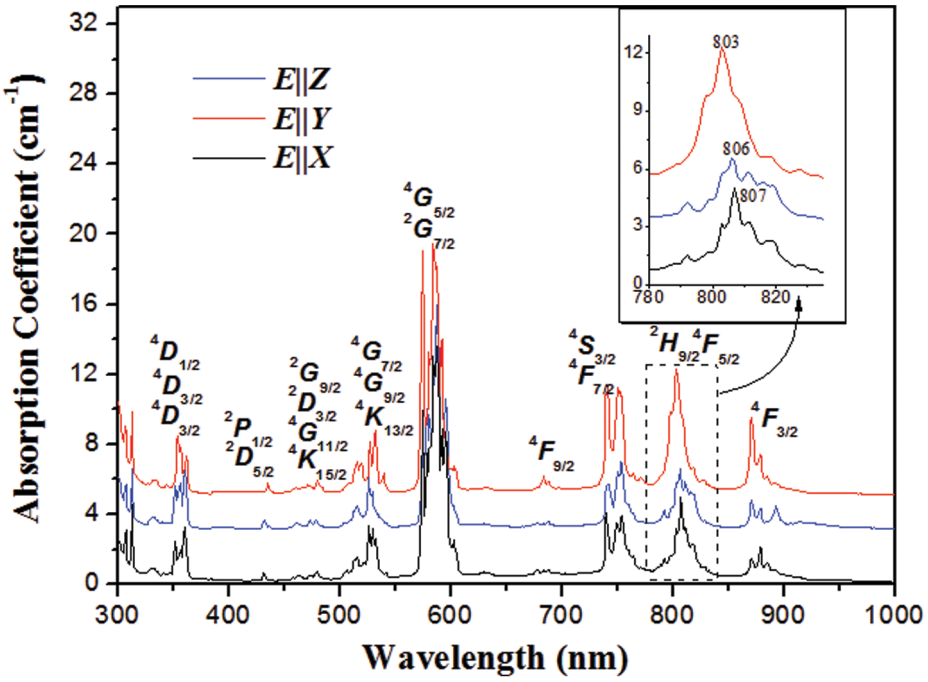

Figure 8. Polarized absorption spectra of Nd^{3+}-doped $KBaGd(WO_4)_3$ crystal at 300 K. The inset shows the spectra in the range of 780 to 840 nm.
doi:10.1371/journal.pone.0040229.g008

Table 2. Comparison of spectral parameters of Nd^{3+}:$KBaGd(WO_4)_3$ with other Nd^{3+}-doped laser crystals.

Crystal	Polarization	Absorption(~805nm)		Emission (~1060 nm)		Disordered	Ref.
		FWHM	σ_a	FWHM	σ_e		
		(nm)	($10^{-20}cm^2$)	(nm)	(10^{-20} cm^2)		
$KBaGd(WO_4)_3$	$E\|\|X$	11	4.5	19	4.5		
	$E\|\|Y$	14	6.9	24	6.5	Yes	
	$E\|\|Z$	19	4.1	19	4.1		
$LiLa(WO_4)_2$	π-polarization	20	2.2	–	8.9	Yes	[24]
	σ-polarization	20	2.8	–	7.8		
$NaY(WO_4)_2$	π-polarization	17	–	≈ 13	–	Yes	[25]
	σ-polarization	17	–	≈ 13	–		
$KBaGd(MoO_4)_3$	unpolarized	9	11.1	24	5.17	Yes	[16]
$BaGd_2(MoO_4)_4$	$E\|\|X$	–	4.3	4	8.6		
	$E\|\|Y$	–	3.3	4	7.2	No	[18]
	$E\|\|Z$	4	17.5	3	19.2		
LaB_3O_6	$E\|\|X$	3	5.0	4	10.2		
	$E\|\|Y$	3	4.5	3	8.3	No	[19]
	$E\|\|Z$	4	5.5	4	7.2		

doi:10.1371/journal.pone.0040229.t002

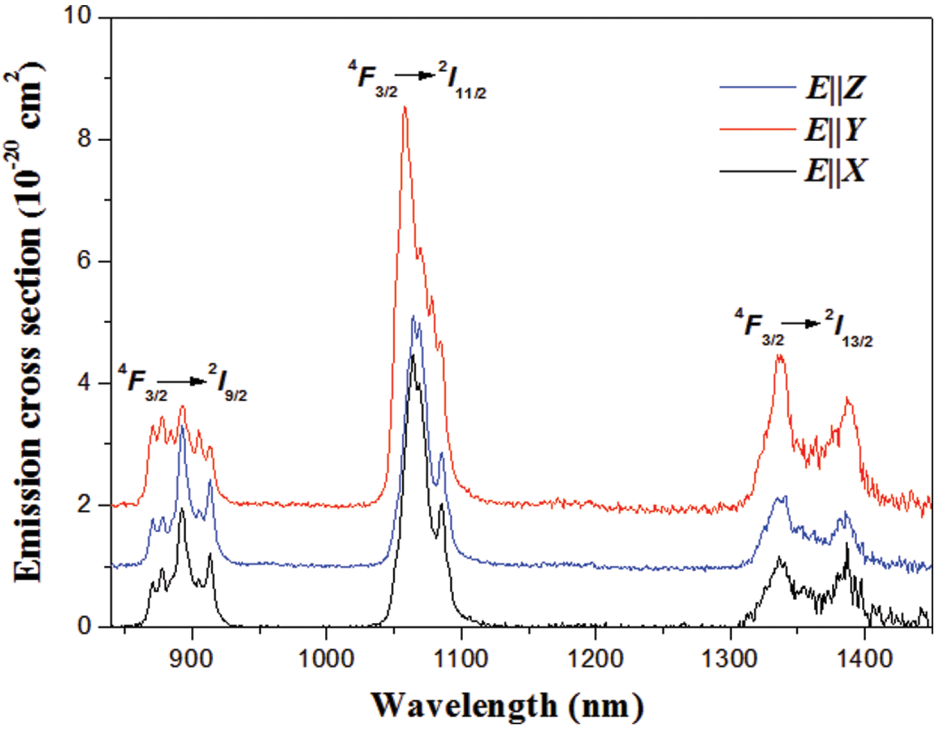

Figure 9. Polarized emission spectra of Nd^{3+}-doped $KBaGd(WO_4)_3$ crystal excited with 805 nm radiation at 300 K.
doi:10.1371/journal.pone.0040229.g009

References

1. Minassian A, Thompson B, Damzen MJ (2003) Ultrahigh-efficiency TEM_{00} diode-side-pumped Nd:YVO_4 laser. Appl Phys B-Lasers Opt 76: 341–343.
2. Razeghi M (1994) High-power laser diodes based on InGaAsP alloys. Nature 369: 631–633.
3. Wang CQ, Chow YT, Reekie L, Gambling WA, Zhang HJ, et al. (2000) A comparative study of the laser performance of diode-laser-pumped Nd:$GdVO_4$ and Nd:YVO_4 crystals. Appl Phys B-Lasers Opt 70: 769–772.
4. Song J, Shen D, Liu A, Li C, Kim NS, Ueda K. (1999) Simultaneous multiple-wavelength cw lasing in laser-diode-pumped composite rods of Nd:YAG and Nd:YLF. Appl Opt 38: 5158–5161.
5. Lu J, Prabhu M, Song J, Li C, Xu J, et al. (2000) Optical properties and highly efficient laser oscillation of Nd:YAG ceramics. Appl Phys B- Lasers Opt 71: 469–473.
6. Giesen A, Hügel H, Voss A, Wittig K, Brauch U, et al. (1994) Scalable concept for diode-pumped high-power solid-state lasers. Appl Phys B 58: 365–372.
7. Cano-Torres JM, Dolores Serrano M, Zaldo C, Rico M, Mateos X, et al. (2006) Broadly tunable laser operation near 2 μm in a locally disordered crystal of Tm^{3+}-doped $NaGd(WO_4)_2$. J Opt Soc Am B 23: 2494–2502.
8. García-Cortés A, Serrano MD, Zaldo C, Cascales C, Strömqvist G, et al. (2008) Nonlinear refractive indices of disordered $NaT(XO_4)_2$ T = Y, La, Gd, Lu and Bi, X = Mo, W femtosecond laser crystals. Appl Phys B-Lasers Opt 91: 507–510.
9. Cascales C, Méndez Blas A, Rico M, Volkov V, Zaldo C (2005) The optical spectroscopy of lanthanides R^{3+} in $ABi(XO_4)_2$ (A = Li, Na; X = Mo, W) and $LiYb(MoO_4)_2$ multifunctional single crystals: Relationship with the structural local disorder. Opt Mater 27: 1672–1680.
10. Cavalli E, Zannoni E, Mucchino C, Carozzo V, Toncelli A, et al. (1999) Optical spectroscopy of Nd^{3+} in $KLa(MoO_4)_2$ crystals. J Opt Soc Am B 16: 1958–1965.
11. Li H, Zhang L, Wang G (2009) Growth, structure and spectroscopic characterization of a new laser crystals Nd^{3+}:$Li_3Ba_2Gd_3(WO_4)_8$. J Alloy Compd 478: 484–488.
12. Sheldrick GM (2008) A short history of it SHELX. Acta Cryst A 64: 112–122.
13. Pujol MC, Rico M, Zaldo C, Solé R, Nikolov V, et al. (1999) Crystalline structure and optical spectroscopy of Er^{3+}-doped $KGd(WO_4)_2$ single crystals. Appl Phys B: Lasers Opt 68: 187–197.
14. Belruss V, Kalnajs J, Linz A, Folweiler RC (1971) Top-seeded solution growth of oxide crystals from non-stoichiometric melts. Mater Res Bull. 6: 899–905.
15. Kaminsky W (2007) From CIF to virtual morphology using the WinXMorph program. J Appl Crystallogr 40: 382–385.
16. Meng X, Lin Z, Zhang L, Huang Y, Wang G (2011) Structure and spectral properties of Nd^{3+}-doped $KBaGd(MoO_4)_3$ crystal with a disorder structure. CrystEngComm 13: 4069–4073.
17. Li H, Wang G, Zhang L, Huang Y, Wang G (2010) Growth and structure of Nd^{3+}-doped $Li_3Ba_2Y_3(WO_4)_8$ crystal with a disorder structure. CrystEngComm 12: 1307–1310.
18. Zhu H, Chen Y, Lin Y, Gong X, Luo Z, et al. (2007) Polarized spectral properties and laser demonstration of Nd^{3+}:$BaGd_2(MoO_4)_4$ cleavage crystal. J Opt Soc Am B 24: 2659–2665.
19. Chen Y, Lin X, Luo Z, Huang Y (2004) Polarized spectral analysis of Nd^{3+} ions in LaB_3O_6 biaxial crystal. Chem Phys Lett 397: 282–287.
20. Aull B, Jenssen H (1982) Vibronic interactions in Nd: YAG resulting in nonreciprocity of absorption and stimulated emission cross sections. IEEE J Quantum Electron 18: 925–930.
21. Judd BR (1962) Optical absorption intensities of rare-earth ions. Phys Rev 127: 750–761.
22. Ofelt GS (1962) Intensities of crystal spectra of rare-earth ions. J Chem Phys 37: 511–520.
23. Korotkov AS, Atuchin VV (2010) Accurate prediction of refractive index of inorganic oxides by chemical formula. J Phys Chem Solids 71: 958–964.
24. Huang XY, Fang Q, Yu QM, Lü XD, Zhang LZ, et al. (2009) Thermal and polarized spectroscopic characteristics of Nd^{3+}:$LiLa(WO_4)_2$ crystal. J Alloy Compd 468: 321–326.
25. Zhou WL, Zhang XX, Chai BHT. (1997) Laser oscillation at 1059 nm of a new laser crystal: Nd^{3+} doped $NaY(WO_4)_2$. OSA Trends in Optics and Photonics Series 10: 451–454.